Available online at www.sciencedirect.com
ScienceDirect
Energy Reports 9 (2023) 221–229
www.elsevier.com/locate/egyr

2022 9th International Conference on Power and Energy Systems Engineering (CPESE 2022), Doshisha University, Kyoto, Japan, 9–11 September 2022

Fault current limitation control of multiple distributed renewable generations under unbalanced conditions

Hongwei Fang[a,*], Ziyan Li[a], Xuanjie Zhang[a], Junjie Xiong[b]

[a] *School of Electrical and Information Engineering, Tianjin University, Tianjin, 300072, China*
[b] *Electric Power Research Institute of State Grid Jiangxi Electric Power Co., Ltd, Jiangxi Province, 330096, China*

Received 20 October 2022; accepted 26 October 2022
Available online xxxx

Abstract

For multiple distributed generation units (DG unit) parallel system, excessive fault current has adverse effects on the safe and stable operation of the utility grid. As a result, a fault current limitation control of multiple DG units is developed in this paper to limit the fault current of related fault branch and ride through the associated fault conditions. The injection fault current amplitude and phase angle of each DG unit for grid-side converter are controlled through the point of common coupling (PCC) voltage support and fault current limitation to limit the total current amplitude at the corresponding fault location. The validity of the proposed control strategy has been verified by simulation and hardware-in-loop (HIL) experiment results.

Peer-review under responsibility of the scientific committee of the 9th International Conference on Power and Energy Systems Engineering, CPESE, 2022.

Keywords: Fault ride-through (FRT); Fault current limitation; Distributed renewable generation; Voltage support

1. Introduction

In recent years, the wide use of renewable energy like wind energy and solar energy has become a feasible method to alleviate the energy crisis and environmental problems. As an effective way to realize the active distributed network, microgrid (MG) can help to solve the grid connection problem of a large number and diverse types of distributed generation units (DG units). Most of the DG units are connected to MG through grid-side converter (GSC). When multiple converters are running in parallel, the characteristics of power grid during fault and the fault ride through control strategy of converters are particularly important [1]. Compared with balanced faults, unbalanced grid faults account for a larger proportion in grid. When an unbalanced fault occurs, the GSC current may be distorted and resulting in more serious stability problems. Also, unbalanced faults will also lead to the sharp deterioration of power quality, including injected power ripple and current harmonics [2]. Therefore, the control for unbalanced faults is particularly important in multiple distributed renewable generations.

* Corresponding author.
E-mail address: hongwei_fang@tju.edu.cn (H. Fang).

https://doi.org/10.1016/j.egyr.2022.10.420

Peer-review under responsibility of the scientific committee of the 9th International Conference on Power and Energy Systems Engineering, CPESE, 2022.

For the multiple DG units, the master–slave control and centralized control have high requirements for the master control unit and central controller, while the inverters in decentralized logic control have the same control status, in which droop control and virtual synchronous generator control are more widely studied [3]. In [4], an adaptive virtual impedance approach is developed to improve power distribution accuracy. And a modified droop control strategy is utilized to realize the power distribution of various converters with different fault degrees. A two-layer hierarchical control strategy is proposed in [5]. Voltage and current control loops, classic droop control loops, and virtual impedance control loops are all part of the main control layer. The sub control layer is a negative sequence component droop control. A hybrid control method is proposed by combining passive switching function and frequency droop control in [6]. Besides the droop control and virtual synchronous generator control, some fault ride through schemes based on specific control objectives have also been investigated. Ref. [7] has proposed a strategy to keep the power angle and other variables in memory during the fault period to deal with the voltage phase shift during the fault period of droop control or virtual synchronous machine control. Ref. [8] proposes a comprehensive autonomous coordinated control scheme that can meet the maximum asymmetric voltage support with voltage, current, and power constraints being considered.

In order to limit the short-circuit fault current, grid splitting operation and bus splitting operation, or series reactor and high short-circuit impedance transformer are usually used. However, these measures reduce the stability and reliability of power system operation and have a great impact on the normal operation of system [9]. Thus, in order to improve the utilization of DG units, ensure the stable operation of the power grid during the fault period, and improve its transmission quality and efficiency, a fault current limitation control (FCLC) for fault ride through multiple distributed renewable generations under unbalanced conditions is proposed in this paper. Simulation and hardware-in -loop (HIL) experiments show that the proposed strategy can reduce the total fault current at the fault points by changing the amplitude and phase of the fault current of each DG unit through the control of converters.

2. PCC voltage support control

The equivalent structural diagram of MG connected to utility grid is shown in Fig. 1. Different distributed generation units are connected to PCC through grid-side inverter and LCL filter. The amplitudes and phase angles of fault currents injected by microgrid and utility grid, are represented by I_t, I_g and θ_t, θ_g respectively. I_f and θ_f are the amplitude and phase angle of the total fault current at the fault branch. The joint fault current is composed of the fault current injected by the microgrid and the utility grid. The MG injection current is composed of those of each DG unit.

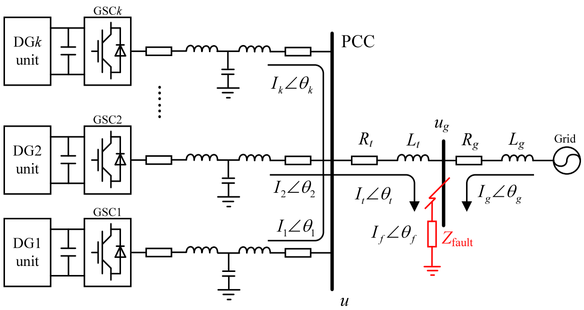

Fig. 1. Structural diagram of microgrid connected to utility grid.

This work proposes a fault ride through control approach based on fault current limitation control to increase the utilization of DG units, transmission quality and efficiency and grid stability during fault conditions.

In case of unbalanced fault conditions, the over-voltage or low-voltage protection scheme at PCC voltage is achieved as [10]:

$$\begin{cases} U_{\max} = \max\{U_a, U_b, U_c\} \leq U_{\max}^{\text{set}} \\ U_{\min} = \min\{U_a, U_b, U_c\} \geq U_{\min}^{\text{set}} \end{cases} \tag{1}$$

where U_a, U_b, U_c are the PCC voltage amplitudes. $U_{\max}^{\text{set}}$ and $U_{\min}^{\text{set}}$ are the set maximum and minimum limit of the three-phase PCC voltage amplitudes (usually, 0.9–1.1p.u.).

The minimum and maximum values of the three-phase PCC voltage during the fault are:

$$\begin{cases} U_{\min} = \min(U_a, U_b, U_c) = \sqrt{(U^+)^2 + (U^-)^2 + 2(U^+)(U^-)\lambda_{\min}} \\ U_{\max} = \max(U_a, U_b, U_c) = \sqrt{(U^+)^2 + (U^-)^2 + 2(U^+)(U^-)\lambda_{\max}} \end{cases} \tag{2}$$

where $\lambda_{\min}$ and $\lambda_{\max}$ can be expressed as:

$$\begin{cases} \lambda_{\min} = \min\left(\cos(\gamma), \cos(\gamma - \frac{2\pi}{3}), \cos(\gamma + \frac{2\pi}{3})\right) \\ \lambda_{\max} = \max\left(\cos(\gamma), \cos(\gamma - \frac{2\pi}{3}), \cos(\gamma + \frac{2\pi}{3})\right) \end{cases} \tag{3}$$

in which, $\gamma = \varphi^+ - \varphi^-$.

The amplitudes of maximum reference values and minimum reference values of the PCC voltage are determined by the set maximum and minimum limits of the PCC voltage as:

$$\begin{cases} U_{\min}^{\text{ref}} = U_{\min}^{\text{set}} \\ U_{\max}^{\text{ref}} = \min(U_{\max}^{\text{set}}, U_{\min}^{\text{set}} + U_{\max} - U_{\min}) \end{cases} \tag{4}$$

Substituting (3) and (4) into (2), the reference values of the three-phase PCC voltage's positive and negative sequence components are expressed as:

$$U_{\text{ref}}^+ = \frac{A + \sqrt{A^2 - B^2}}{2C}, \quad U_{\text{ref}}^- = \frac{A - \sqrt{A^2 - B^2}}{2C}, \quad \textit{where} \begin{cases} A = \lambda_{\max}\left(U_{\min}^{\text{ref}}\right)^2 - \lambda_{\min}\left(U_{\max}^{\text{ref}}\right)^2 \\ B = \left(U_{\min}^{\text{ref}}\right)^2 - \left(U_{\max}^{\text{ref}}\right)^2 \\ C = \lambda_{\max} - \lambda_{\min} \end{cases} \tag{5}$$

3. Fault current limitation control

The following analysis is performed on a parallel system with two DG units to obtain the phase angle reference value of each distributed generation unit's GSC output fault current. Fig. 2 shows the relationship between fault currents and phase angles. In Fig. 2, I_1 and I_2 are the fault currents injected by the GSC, I_g is the fault current injected by the utility grid. And I_f is the total fault current at the fault branch, consisting of I_g, I_1 and I_2. Change the amplitude and phase angle of fault currents injected by two distributed generation units to I_{1_ref}, I_{2_Ref} and θ_{1_ref}, θ_{2_ref}. The total fault current will turn to $I_{\text{f\_new}}$ which consists of I_{g}, I_{1_ref} and I_{2_ref}, and the amplitude is controlled by the amplitude of I_{g}.

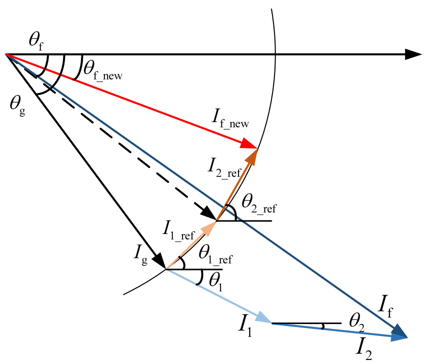

Fig. 2. Relationship between fault currents.

Thus, if there are k distributed generation units in parallel, the corresponding total fault current is expressed as [11]:

$$\vec{I}_{f\_\text{new}}^{+/-} = \vec{I}_g^{+/-} + \sum_{k=1}^{n} \vec{I}_{k\_\text{ref}}^{+/-} \tag{6}$$

where $\vec{I}_{f\_\text{new}}^{+/-}$ is the total fault current at fault branch under FCLC, $\vec{I}_g^{+/-}$ is the fault injection current from utility grid, $\vec{I}_{k\_\text{ref}}^{+/-}$ is the reference value of fault injection current of the k_{th} DG unit.

From Section 2, the reference value of fault injected reactive current of each DG unit can be calculated, and the fault current amplitude at fault point and that injected by the utility grid is controlled to be same as:

$$\begin{cases} \hat{I}_{k\_\text{ref}}^{+/-} = \dfrac{\hat{I}_{q(k)\_\text{ref}}^{+/-}}{\sin(\theta_{k\_\text{ref}}^{+/-})} \\ \hat{I}_{f\_\text{new}}^{+/-} = \hat{I}_g^{+/-} \end{cases} \tag{7}$$

where $\hat{I}_{k\_\text{ref}}^{+/-}$ and $\theta_{k\_\text{ref}}^{+/-}$ are the fault injection current's amplitude and phase angle of the kth DG unit.

Further, (7) can be expressed as:

$$\begin{cases} \hat{I}_g^{+/-}\left[\cos(\theta_{f\_\text{new}}^{+/-}) - \cos(\theta_g^{+/-})\right] = \sum\limits_{k=1}^{n} \hat{I}_{k\_\text{ref}}^{+/-} \cos\left[\pi - \theta_g^{+/-} - \arccos\left(\dfrac{\hat{I}_{k\_\text{ref}}^{+/-}}{2\hat{I}_g^{+/-}}\right)\right] \\ \hat{I}_g^{+/-}\left[\sin(\theta_{f\_\text{new}}^{+/-}) - \sin(\theta_g^{+/-})\right] = \sum\limits_{k=1}^{n} \hat{I}_{k\_\text{ref}}^{+/-} \sin\left[\pi - \theta_g^{+/-} - \arccos\left(\dfrac{\hat{I}_{k\_\text{ref}}^{+/-}}{2\hat{I}_g^{+/-}}\right)\right] \end{cases} \tag{8}$$

where $\theta_g^{+/-}$ and $\theta_{f\_\text{new}}^{+/-}$ are the phase angle of fault injection current of utility and total fault current under FCLC.

From (7) and (8), the positive- and negative-sequence components of phase angle reference values for each DG unit can be expressed as:

$$\theta_{k\_\text{ref}}^{+/-} = \frac{1}{2}\left\{\pi + \arcsin\left[\frac{\hat{I}_{q(k)\_\text{ref}}^{+/-}}{\hat{I}_g^{+/-}} - \sin\left(\theta_g^{+/-} - \Delta\theta\right) - \theta_g^{+/-}\right]\right\} \tag{9}$$

The amplitude reference value and phase reference value of the reactive current infused by the DG units can be obtained, and the PWM signal of each GSC can be obtained through the current control loop. The principal control diagram of FCLC is shown in Fig. 3.

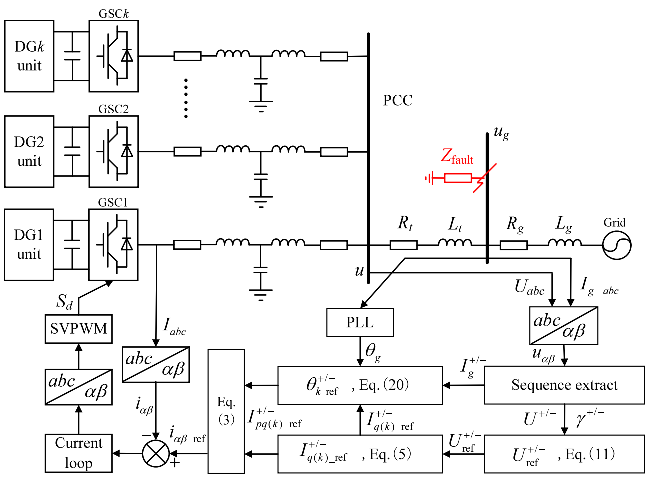

Fig. 3. FCLC's principal control diagram.

The control process is described as follows. The coordinate transformation, positive and negative sequence separation, and phase detection are applied to obtain the PCC voltage. The PCC voltage reference value and the injection reactive current reference value of each DG unit are calculated according to the PCC voltage regulation control, to support the PCC voltage and limit the PCC voltage within the allowable value range. Then, by limiting the total fault current amplitude to the fault current amplitude injected by the utility grid, the phase angle reference value of the fault injection current of each DG unit is obtained. The reference value of the inverter fault injection current in the two-phase static coordinate system can be obtained if the reference value of the reactive component of the inverter injection current and the phase reference value's positive and negative sequence components is determined.

Compared with the current value of the inverter in the two-phase static coordinate system, the PWM control signal can be obtained through the PR controller and Park transformation to control the inverter of each DG unit.

4. Simulation and experimental verification

4.1. FCLC simulation

The simulation model of the parallel system with two GSCs is built, and the results of FCLC and those without FCLC are compared. Table 1 presents the main simulation parameters.

Table 1. Main simulation parameters.

Symbol	Quantity	Value	Symbol	Quantity	Value
L	Inductance of LCL filter	6.42 mH	U_N	Rated grid voltage	311 V
C	Capacitance of LCL filter	15 μF	C_{dc}	DC capacitor	40 μF
R_g/Lg	Line impedance from UG to fault point	0.2 Ω/1.18 mH	S_1	Rated output capacity of GSC1	10 kVA
R_t/Lt	Line impedance from MG to fault point	1.5 Ω/1 mH	S_2	Rated output capacity of GSC1	20 kVA
U_{dc}	DC voltage	700 V	f_s	Switching frequency	10 kHz

The running time is set from 0.05s to 0.25s. The ground fault of phase A occurs at 0.1s, and it is cleared at 0.2s. Fig. 4 shows the three-phase AC voltage and its amplitude at PCC under FCLC and without FCLC. As shown in Fig. 4(a) and Fig. 4(c), the amplitude of phase C's voltage at PCC without FCLC strategy rises to 355 V, and the amplitude of phase B's voltage falls to 260 V, exceeding the upper and lower limitation of PCC voltage. When a fault occurs, the three-phase PCC voltage is controlled within the permissible range by the PCC voltage regulation support control, as shown in Figs. 4(b) and 4(d). The amplitude of phase C's voltage increases to 340 V, and the amplitude of phase B's voltage decreases to 280 V. Thus, the effectiveness of the control strategy in adjusting the three-phase PCC voltage amplitude is verified. The results also show that the PCC voltage is better than that presented in [8].

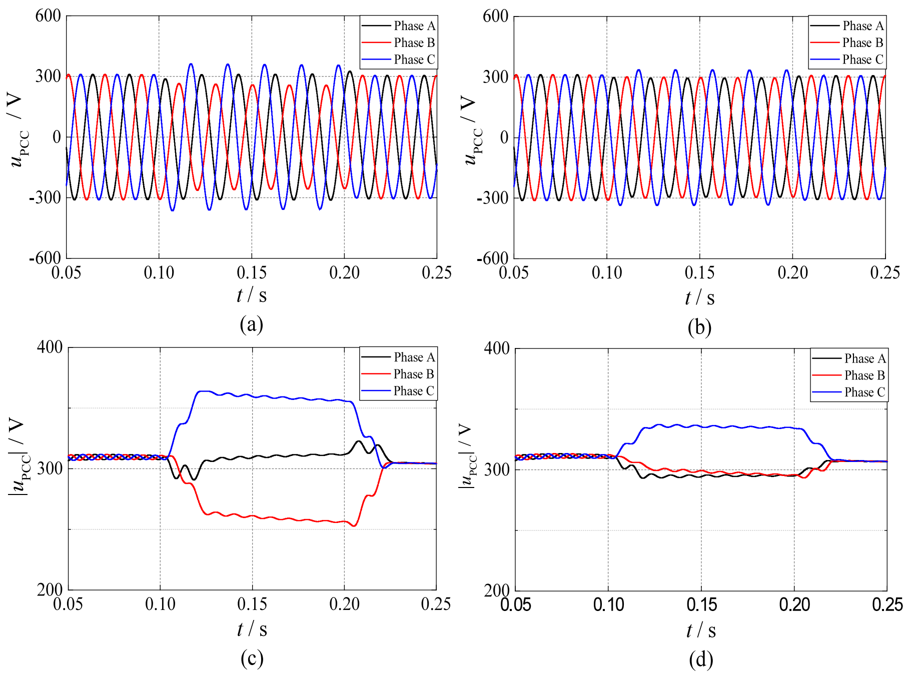

Fig. 4. PCC voltage results with and without FCLC. (a) PCC voltage without FCLC; (b) PCC voltage with FCLC; (c) voltage amplitude without FCLC; (d) voltage amplitude with FCLC.

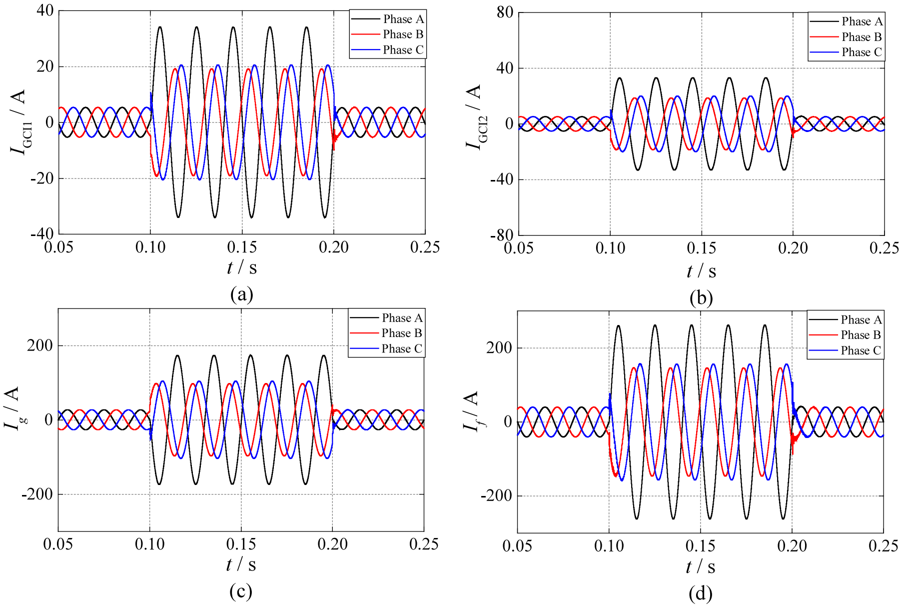

Fig. 5. Fault current without FCLC. (a) GSC1 injection fault current; (b) GSC2 injection fault current; (c)utility grid injection fault current; (d) total fault current at fault bus.

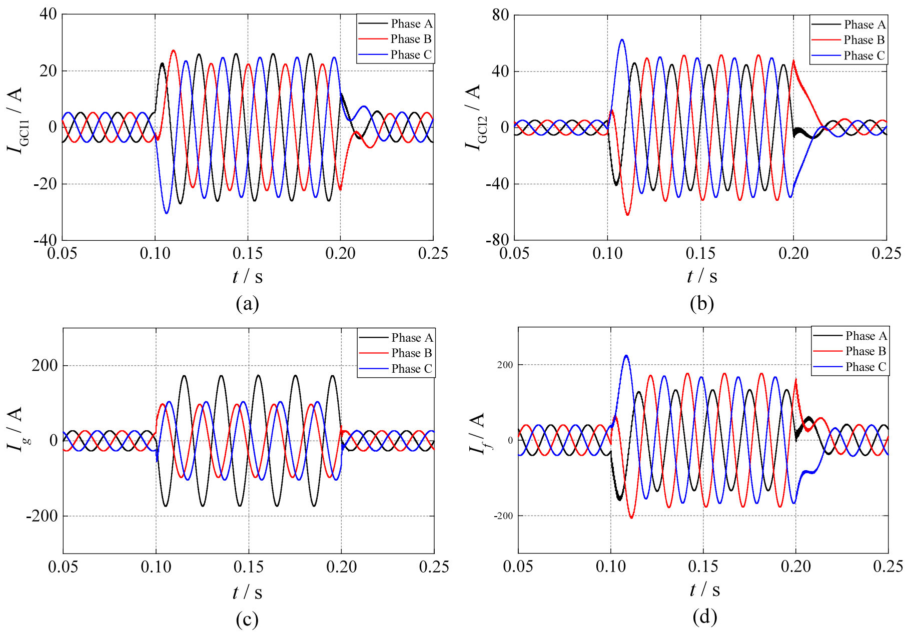

Fig. 6. Fault current with FCLC. (a) GSC1 injection fault current; (b) GSC2 injection fault current; (c) utility grid injection fault current; (d) total fault current at fault bus.

Fig. 5 shows the injection fault currents of the system without FCLC, including GSC1 fault injection current, GSC2 fault injection current, utility grid injection fault current, and the total fault current. When a phase ground fault occurs, the fault injection current amplitude of GSC1 and GSC2 increases to 35 A, the amplitude of the utility grid injection fault current increases to 180 A, and the total fault current rises to about 250 A.

Fig. 6 shows the injection fault current of the system with FCLC. The amplitude of GSC1 injection fault current decreases to 26 A and the phase angle is 20° ahead. The amplitude of GSC2 injection fault current rises to 50

A, and the phase angle lags 20°, the utility grid injection fault current remains unchanged. The total fault current amplitude at the fault bus decreases to 180 A. By changing GSC1 and GSC2 injection fault current's amplitude and phase angle, the amplitude of total fault current is reduced, which has validated the effectiveness of FCLC.

4.2. HIL experiment

The HIL experiment is performed on dSPACE 1104 to further verify the effectiveness and correctness of the proposed FCLC strategy. Fig. 7 presents the experimental platform.

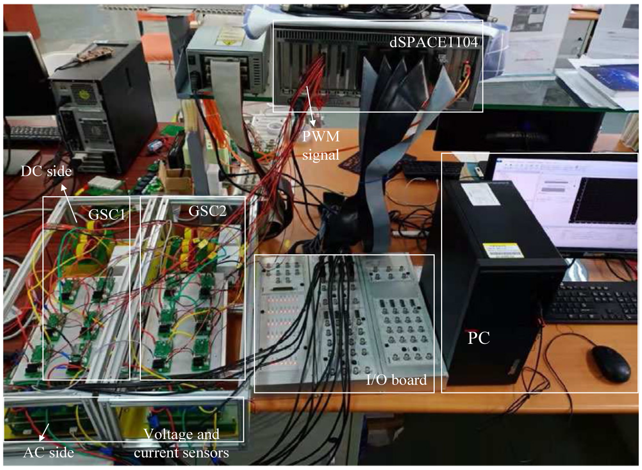

Fig. 7. The HIL experimental platform.

In order to simplify the experiment, the rectification and energy storage of DG units are replaced by DC voltage sources. The main parameters are shown in Table 2.

Table 2. Main parameters in HIL experiment.

Symbol	Quantity	Value	Symbol	Quantity	Value
L_1	GSC1 inductance	4 mH	S_1	Rated output capacity of GSC1	10 kVA
L_2	GSC2 inductance	4 mH	S_2	Rated output capacity of GSC2	15 kVA
C_1	GSC1 capacitance	10 μF	U_N	Rated grid voltage	155 V
C_2	GSC2 capacitance	10 μF	f_s	Switching frequency	5 kHz

During the experiment, a single-phase-ground fault is performed, the single-phase voltage and the faulty phase current at PCC are measured. The voltage and current results with and without FCLC are shown in Fig. 8. As shown in Fig. 8(a) and Fig. 8(c), the single-phase PCC voltage amplitude and faulty phase current reach 55 V and 16 A, respectively. By adopting the FCLC strategy, the voltage and current amplitude are controlled as Fig. 8(b) and Fig. 8(d) shown. Results show that the single-phase PCC voltage amplitude drops to 48 V, and the faulty current amplitude is limited to 11 A. So, it can be found that the experimental and simulation results are basically consistent, which also verifies the correctness of the theoretical analysis and the effectiveness of the proposed FCLC method.

5. Conclusion

In this paper, the short-circuit fault problem of multiple renewable DG units connected to the utility grid is analyzed. The PCC voltage support control is used to limit the PCC voltage during the fault conditions. And the fault current limitation control is proposed to change each DG unit's current amplitude and phase angle to limit the corresponding current of fault branch. Compared with the power system that without the FCLC strategy, the proposed FCLC strategy makes the three-phase voltage at PCC point controlled within the allowable range, effectively reduces the total fault current amplitude at the fault point and avoids the damage or even more serious consequences of relevant equipment in the fault line. The effectiveness of the proposed control approach has been

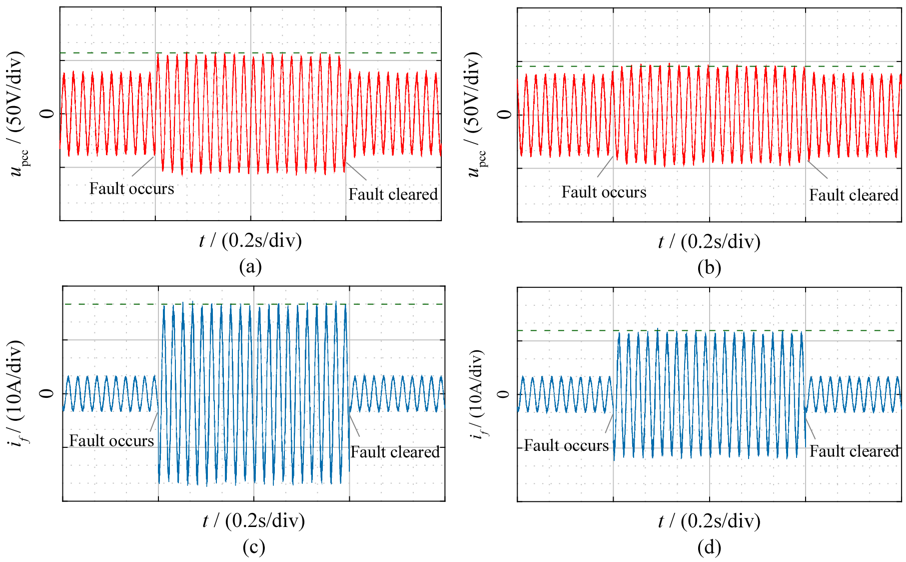

Fig. 8. Voltage and current results with and without FCLC. (a) single-phase PCC voltage without FCLC; (b) single-phase PCC voltage with FCLC; (c) faulty phase current without FCLC; (d) faulty phase current with FCLC.

verified by both simulation and experimental results. It can be found that the proposed control method can be used in renewable energy power generations to increase the system reliability.

Declaration of competing interest

The authors declare that they have no known competing financial interests or personal relationships that could have appeared to influence the work reported in this paper.

Data availability

No data was used for the research described in the article.

Acknowledgments

The work is supported by a grant from National Natural Science Foundation of China (No. 51877148) and Tianjin Research Innovation Project for Postgraduate Students, China (2021YJSS019).

References

[1] Fang Hongwei, Zhang Xuanjie. Improvement of low-voltage-ride-through capability for wave energy conversion system. IEEE Trans Ind Electr 2022;69(8):8123–33.
[2] Shabestary Masoud M, Abdol-Rady Yasser, Mohamed I. Asymmetrical ride-through and grid support in converter-interfaced DG units under unbalanced conditions. IEEE Trans Ind Electron 2019;66(2):1130–41.
[3] Fang Hongwei, Yu Zhiwei. Improved virtual synchronous generator control for frequency regulation with a coordinated self-adaptive method. CSEE J Power Energy Syst 2020;1–10.
[4] Chen Jie, Liu Ming-ao, Chen Xin, et al. Wireless parallel and circulation current reduction of droop-controlled inverters. Trans China Electrotech Soc 2018;33(7):1450–60.
[5] Zhao Xin, Guerrero Josep M, Savaghebi Mehdi, et al. Low-voltage ride-through operation of power converters in grid-interactive microgrids by using negative-sequence droop control. IEEE Trans Power Electron 2017;32(4):3128–42.
[6] Li Canbing, Liu Xubin, Sun Kai, et al. A hybrid control strategy to support voltage in industrial active distribution networks. IEEE Trans Power Deliv 2018;33(6):2590–602.
[7] Fang Zhixue, Su Jianhui, Wang Huafeng. Low voltage ride through control strategy for microgrid inverter. Autom Electr Power Syst 2019;43(2):143–9+161.
[8] Shabestary Masound M, Abdol-Rady Yasser, Mohamed I. Analytical expressions for multiobjective optimization of converter-based DG operation under unbalanced grid conditions. IEEE Trans Power Electron 2017;32(9):7284–96.

[9] Wu Shouyuan, Jing Ping, Dai Chaobo, et al. Fault current limiting technology and its new progress. Power Grid Technol 2008;32(24):23–32.
[10] Liu Xubin, Li Canbing, Shahidehpour Mohammad, et al. Fault current hierarchical limitation strategy for fault ride-through scheme of microgrid. IEEE Trans Smart Grid 2019;10(6):6566–79.
[11] Zhao Xin, Guerrero Josep M, Savaghebi Mehdi, et al. Low-voltage ride-through operation of power converters in grid-interactive microgrids by using negative-sequence droop control. IEEE Trans Power Electron 2017;32(4):3128–42.